Cancer Immunology, Immunotherapy (2025) 74:150
https://doi.org/10.1007/s00262-025-04004-4

RESEARCH

MS275 induces tumor immunosuppression by upregulating PD-L1 and enhances the efficacy of anti-PD-1 immunotherapy in colorectal cancer

Deng Tang[1] · Zhigang Mao[2] · Sihan Chen[1] · Mi Su[1] · Siqi Lan[1] · Ruiting Yan[1] · Qi Xiang[1] · Xianxian Zhao[1] · Ji Zhang[1] · Yufang Wang[1]

Received: 20 March 2024 / Accepted: 26 February 2025 / Published online: 17 March 2025

Abstract

The histone deacetylase inhibitor MS275 (Entinostat) demonstrates anti-tumor effects against various types of solid tumors in vitro. But its effectiveness in clinical trials is limited. The underlying reasons remain to be determined. The purpose of this study was to explore how to enhance the anti-tumor effects of MS275 in colorectal cancer (CRC). Our data showed that MS275 inhibited CRC cell proliferation and induced apoptosis, irrespective of gene mutation status. However, MS275 did not effectively suppress tumor growth in the AOM-DSS CRC model as observed in vitro. MS275 decreased CD3+T cell tumor infiltration and created an immunosuppressive microenvironment in the AOM-DSS CRC model. MS275 also decreased the percentage of CD8+T cells while increasing the percentage of CD4+T cells in mesenteric lymph nodes. Reshaping tumor immune response may contribute to the less pronounced anti-tumor effect of MS275 observed in vivo compared to in vitro. Further study showed that the increased PD-L1 expression in CRC both in vivo and in vitro following MS275 treatment. Moreover, the anti-tumor effects of MS275 were enhanced by combining it with an anti-PD-1 antibody. This combination treatment also increased CD8+T cell tumor infiltration in the AOM-DSS CRC model, thereby leading to an anti-tumor immune response. Therefore, the combination of MS275 and anti-PD-1 immunotherapy represents a potential strategy for low PD-L1 expression tumors and should be considered a promising treatment approach for colon cancer.

Keywords HDACi · MS275 · PD-L1 · Colorectal cancer

Introduction

Colorectal cancer (CRC) is the third most commonly diagnosed cancer as well as the third leading cause of cancer-related deaths. Environmental risk factors including lifestyle, together with the inherited genetic background, may lead to the development of the tumor [1].

Although genetic mutations (K-Ras, ß-catenin, p53, et.al) undoubtedly play a significant role in CRC initiation and development, CRC progression is also driven by epigenetic modifications, including DNA methylation, histone protein modifications, and non-coding RNA-mediated gene silencing. Histone deacetylase (HDAC) plays a critical role in the development of cancer by reversibly modulating the acetylation status of histone and nonhistone proteins [2]. Recent studies suggest that HDACs, particularly HDAC-1, -2, -3 and -8 [3] are overexpressed in CRC and their increased expression is correlated with a poorer prognosis [4]. This highlights the potential of HDACs as therapeutic targets in CRC.

Histone deacetylase inhibitors (HDACIs) may block tumor cell proliferation by restoring the balance of histone acetylation, thus resulting in proper gene expression. They can induce growth arrest, apoptosis, and/or differentiation of

Deng Tang, Zhigang Mao and Sihan Chen have contributed equally to this work.

✉ Ji Zhang
zhangj@scu.edu.cn

✉ Yufang Wang
wangyufang@scu.edu.cn

[1] West China School of Basic Medical Science and Forensic Medicine, Sichuan University, Chengdu 610041, Sichuan, People's Republic of China

[2] Department of Laboratory Medicine, West China Hospital, Sichuan University, Chengdu 610041, Sichuan, People's Republic of China

transformed cells both in vitro and in vivo [2]. Furthermore, HDACIs have been shown to modulate the tumor immune microenvironment [5], affecting immune responses such as antigen presentation, T cell activation, and differentiation of regulatory T cells (Tregs). This immunomodulatory effect suggests that HDACIs could also impact the efficacy of immunotherapy in cancer.

However, initial clinical trials employing HDACIs as monotherapy against CRC revealed either limited responses or no response at all [6]. These trials were also hindered by clinical adverse events due to HDACIs toxicity, which was mainly attributed to global histone acetylation, a phenomenon not limited to cancer cells [1]. Therefore the search for HDAC inhibitors with high specificity is the main direction for the treatment of targeted HDACs.

N-(2-aminophenyl)-4-[*N*-(pyridine-3yl-methoxy-carbonyl) aminomethyl] benzamide (MS-275) is a class I histone deacetylase inhibitor (HDAC) that selectively targets HDAC1, HDAC2, and HDAC3 [7]. MS275 has shown promising results, especially against advanced breast cancer [8] and colon cancer in vitro [9]. However, clinic phase trials indicate that neither monotherapy nor combination therapy with MS275 was well tolerated and showed no evident activity in metastatic CRC [6]. Further studies of MS275 are warranted to enhance its efficacy through combination with other novel agents, like PD-1/PD-L1 inhibitors.

In our study, we observed that MS275 inhibits CRC proliferation both in vitro and in vivo. However, it also suppresses the anti-tumor immune microenvironment by upregulating the expression of PD-L1. Additionally, we found that there is a synergistic effect with MS275 and PD-1 immunotherapy in the treatment of CRC. Combining MS275 with immunotherapy may hold greater promise for improving treatment for CRC.

Materials and methods

Cell lines and reagents

The human colon cancer cell lines $HCT116^{Mut}$, $HCT116^{WT}$, $DLD1^{Mut}$ and $DLD1^{WT}$, HT29 and SW480 were kindly provided by Dr. Kevin Haigis (Beth Israel Deaconess Medical Center, Boston, USA). $DLD\text{-}1^{Mut}$ and $HCT116^{Mut}$ cell lines contain the KRAS G13D mutation; $DLD\text{-}1^{WT}$ and $HCT116^{WT}$ are their isogenic cell lines carrying the wildtype KRAS. The mouse colon cancer cell line CT26 was purchased from Kunming Cell Bank (KCB, China). All cells were cultured in high-glucose DMEM with 5% FBS, and maintained under humidified conditions (37 °C, 5% CO_2), and continuous culture did not exceed 2 months. STR genotyping of each cell line is performed and compared to the STR profiles of known standard cell lines from the American Type Culture Collection (ATCC). MS275 was purchased from MCE (HY-12163, USA). InVivoPlus anti-mouse PD-1 (CD279) was purchased from Bio X cell (#BE0146, Lebanon, NH, USA).

Antibodies

The following antibodies were used for Western blotting: anti-STAT3(#9139), anti-p-STAT3(#9145), anti-cleaved-PARP(#5625), anti-PD-L1(#13684), anti-rabbit antibody(#7074), all of these were purchased from Cell Signaling Technology (Danvers, MA, USA). Anti-HDAC1(sc-81598) and anti-HDAC3(sc-17795) were purchased from Santa Cruz, Anti-HDAC2(abs136328) and goat anti-mouse antibody from Absin, Pan Acetylation Monoclonal antibody(66289) from Proteintech. Anti-β-actin(#A2228) was purchased from Sigma-Aldrich. The following antibodies were used for immunohistochemistry (IHC): anti-F4/80(#70076), anti-CD3(#78588), anti-Arginase-1(#93668), anti-iNOS(#13120), anti-CD8(#98941), and Brdu(#5292), all were purchased from Cell Signaling Technology (Danvers, MA, USA).

Cell proliferation assays

MTS assay was performed using the CellTiter 96 Aqueous One Solution Cell Proliferation Assay kit (Promega, Madison, WI, USA). Briefly, cells were seeded into 96-well plates at 75% confluence and incubated overnight. The cells were treated with MS275 for 48 h, and an equal amount of DMSO was added to the control. The cell viability was measured using the MTS assay.

A BrdU staining procedure was employed to assess the proliferation of intestinal epithelium in a mouse model of colorectal cancer. BrdU(100 mg/kg) was administered via intraperitoneal injection to the mice two hours prior to sacrifice. After fixation and embedding of the intestinal tissue, IHC was performed according to protocol.

Apoptosis analysis

Apoptosis in colorectal cancer cells treated with MS275 for 48 h was analyzed using an Annexin V-FITC Apoptosis Detection Kit II (BD). The results were measured using the BD Accuri C6. The percentage of apoptosis was then calculated based on the cells in the region of Q2 and Q4.

The assessment of apoptosis was conducted via TUNEL staining of the intestinal epithelium in a mouse model of colorectal cancer.

RNA and RT-qPCR

RNA was extracted using TRIzol (#15596026, Thermo Fisher Scientific), and cDNA was synthesized using a GoScript™ Reverse Transcription Mix (A2790, Promega). The qPCR assays were performed using GoTaq® qPCR Master Mix (A6002, Promega) and a QuantStudioTM 5 Real-Time PCR System (Thermo Fisher Scientific). GAPDH was used simultaneously as the internal control. The data was analyzed using the 2–ΔΔCt method. Primer sequences for the following mouse genes are listed: Mus-PD-L1-F: 5′-GAGTGCAGATTCCCTGTAGAAC-3′; Mus-PD-L1-R: 5′-CTCTCCTGCCACAAACTGAA-3′; Mus-GAPDH-F: 5′-TCTTGGGCTACACTGAGGAC-3′; Mus-GAPDH-R: 5′-CATACCAGGAAATGAGCTTGA-3′. Primer sequences for the following homo genes are listed: Homo-PD-L1-F:5′-ACCAGCACACTGAGAATC AAC-3′; Homo-PD-L1-R:5′-GGTAGTTCTGGGATGACC AATTC-3′; Homo-GAPDH-F: 5′-GGTGTGAACCATGAG AAGTATGA-3′; Homo-GAPDH-R: 5′-GAGTCCTTCCAC GATACCAAAG-3′.

Western blotting

Cell lysis buffer (100 mM NaCl, 10 mM EDTA (pH 8.0), 50 mM Tris–Cl (pH 8.0) and 0.5% (v/v) Triton X-100 with EDTA-free complete protease and phosphatase inhibitors (KGB5105-10, KeyGEN BioTech) was used for protein extraction. The lysates were separated on a 10% SDS-PAGE gel and transferred onto PVDF membranes. The targets were detected using the ImageQuant LAS 4000 (GE Healthcare Life Sciences). Actin was used as the loading control.

AOM-DSS CRC mouse model

Male Balb/c mice were placed in an SPF-grade standard environment for one week of adaptation feeding. To establish the CRC mouse model, an intraperitoneal injection of azoxymethane (AOM) (10mg/kg) was administered on the first day. After 7 days, mice were provided with drinking water containing 1.5% dextran sulfate sodium (DSS) for a week. Followed by regular drinking water for another two weeks, constituting one cycle of water administration. A total of three cycles of AOM-DSS treatment were performed. Four weeks after the completion of the AOM-DSS cycles, mice were orally administered with MS275 (20 mg/kg) per day, lasting for 21 days. The colons were collected, and the tumors were counted and measured.

This experimental procedures were approved by the Institutional Animal Care and Use Committee of Sichuan University. All animal housing and experiments were conducted in strict accordance with the institutional guidelines for care and use of laboratory animals.

Orthotopic CRC models

Both immunodeficient (nude) mice and immunocompetent (Balb/c) mice were obtained from Laboratory animal center, Sichuan University and raised under specific pathogen-free (SPF) conditions. Animal experiments in this study were approved by the Animal Experiment Committee of Sichuan University. Anesthesia was induced isoflurane gas. Transplantation was performed under a zoom stereomicroscope (Carl Zeiss, Oberkochen, Germany) by inject 2.5×10^6 CT26 cells in 50 µl PBS into the triangle of the cecum mesentery for each mouse. Approximately five days post-operation, a smooth mass was palpated in the left lower abdomen of the mice, indicating successful in situ transplantation tumor surgery. Subsequently, the mice were randomly allocated to groups for the specified treatments.

Isolation of mesenteric lymph nodes (MLN) Cells

The MLN were placed in sterile Petri dishes containing PBS-HEPES (4 °C) and minced with scraping using a sterile scalpel blade. The minced MLN were filtered through a 70 µm filter, pieces of tissue were then crushed on the filters, and were washed twice with PBS-HEPES (4 °C). Contaminating red blood cells were lysed, the single MLN cells were resuspended in RPMI supplemented with 10% heat-inactived fetal calf serum for FACS or Elisa analysis.

Immunochemistry (IHC)

Paraffin-embedded tissues were used for IHC staining. After deparaffinized in xylene for 10 min, the slides were immersed in 3% H_2O_2 for 20 min to block the endogenous peroxidase and blocked in goat serum blocking solution for 30 min. After being incubated at 4 °C overnight with primary antibodies, the slides were incubated with secondary HRP-conjugated antibodies for 30 min at RT. The primary antibodies were shown above. IHC staining was examined with microscopy. The positive staining score from 0 to10 was used to assess different antibody stained tissue sections by two trained senior pathologists in a double-blind independent approach to establish reference values.

Elisa

Supernatants of cultured cells were collected and centrifuged. ELISA kits for mouse TNF-α (VAL609, NOVUS) and mouse IFN-γ (VAL607, NOVUS) were used according to the manufacturer's instructions. The absorbance of the samples was measured using Synergy™ HT microplate

reader (BioTek). The concentration of cytokines in the supernatants was calculated based on the standard curve generated using the provided cytokines standard.

Flow cytometry analysis

The following mouse antibodies were used for flow cytometry analyses: Anti-PD-L1 PE (BD, 557924), anti-CD3e PerCP-CyTM5.5 (BD, 551163), anti-CD4 FITC (BD, 553046), and anti-CD8 alpha PE (BD, 553046). Gates were determined using isotype control Ab staining. Data were acquired with BD C6 flow cytometry.

Plasmid construction and transfection

The plasmid vector expressing short hairpin RNA (shRNA) targeting the sequences of the HDAC1 gene (GCAAGA ACTCTTCCAACTT), HDAC2 gene (CTATTATCTCAA AGGTGAT), HDAC3 gene (GCATTACGGTCTCTATAA GAA), and a negative control (TTCTCCGAACGTGTC ACGT), were synthesized and cloned into GV102 (SD11) vector with BsmBI sites (purchased from Shanghai Genechem Co., Ltd.), recombinant vector was detected by DNA sequencing. The final products were then transfected into Escherichia coli. DH5α followed by extraction with Endofree plasmid Mega kit(Qiagen, Hilden, Germany) obtained shRNA- HDAC1, HDAC2, and HDAC3 plasmid.

Plate CRC cells in a 6-well plate at 80% confluence and incubate overnight. Prepare a transfection mixture by combining 1 µg of plasmid, 3 µl of transfection reagent, and 100 µl of serum-free DMEM medium. Mix gently, then add the mixture drop by drop to the cell culture plate. Gently swirl to ensure even distribution and incubate the cells for 72 h, then harvest cells for analysis.

Statistical analysis

The data were analyzed by two-tailed Student's t test or ANOVA using GraphPad Prism software (La Jolla, CA). Comparisons between groups are presented as the mean ± SEM. Values of $p < 0.05$ were considered statistically significant.

Results

MS275 inhibits proliferation of colorectal cancer cells and induces apoptosis

MS275 is a class I selective HDACi that targets HDAC1, HDAC2 and HDAC3 in cells. MS275 (1 µM, 2.5 µM and 5 µM) was applied to CRC cells for 48 h, the level of pan acetylation of protein was significantly increased. Western Blot assay showed that MS275 dose-dependently decreased the intracellular HDAC3 protein expression level, while not affecting the HDAC1 and HDAC2 protein expression levels (Fig. 1A).

Two pairs of cell lines, HCT116^{Mut} and HCT116^{WT}, as well as DLD-1^{Mut} and DLD-1^{WT}, shared the same genetic background but differed in KRAS mutation status. DLD-1^{Mut} showed more sensitivity to MS275 compared to DLD-1^{WT} (Fig. 1B), while the reverse was observed in the HCT116 cell line pair (Fig. 1C). MS275 inhibited cell proliferation regardless of KRAS mutation status. Additionally, we treated a panel of colorectal cell lines with MS275 at indicated concentrations (0.1–10 µM) for 48 h. The MTS assay revealed a dose-dependent reduction in cell viability (Fig. 1D). Among these cell lines, HCT116^{Mut}, DLD1^{Mut}, and SW480 carry active KRAS mutations (G13D), whereas HT29 harbors BRAF V600 mutations. Interestingly, the sensitivity to the drug did not correlate with gene mutations across different cell lines.

We evaluated the percentage of apoptosis induced by MS275 using the Annexin V-PI staining assay, with the results shown in Fig. 1E. Following treatment with MS275, 31.8% apoptosis was observed in the HCT116^{Mut} cell lines. Furthermore, MS275 induced apoptosis in a dose-dependent manner. Additionally, cleavage of PARP, a hallmark of apoptosis, was observed after treatment with the indicated concentrations of MS275 in both HCT116^{Mut} and HCT116^{WT} cell lines (Fig. 1F). The induction of apoptosis by MS275 was further confirmed in a panel of CRC cell lines (Fig. 1G).

MS275 showed anti-tumor activity against colon cancer in vivo

To elucidate the tumor-suppressing effect of MS275 in vivo, we established a classical mouse colorectal cancer model (see Materials and Methods section). Four weeks after the completion of the AOM- DSS cycle, mice received MS275 at a dose of 20 mg/kg via gavage. After 3 weeks of treatment, the mice were euthanized and their colons were examined, shown in Fig. 2A.

Following treatment of colorectal cancer mice with MS275, the total size of all tumors in the colon segment did not show a significant reduction (Fig. 2B). However, the number of colon tumors decreased by 23.6% compared to that of the control group (Fig. 2C). To evaluate the proliferation of the intestinal epithelium, BrdU (100 mg/kg) was administered to the mice by intraperitoneal injection two hours before sacrifice. IHC was used to evaluate the positive staining of BrdU in the intestinal tumors of mice from each group. The results showed that the intensity of local BrdU staining in tumors of mice in the control group was higher than that in the MS275-treated group (Fig. 2D), indicating that MS275 could inhibit tumor cell

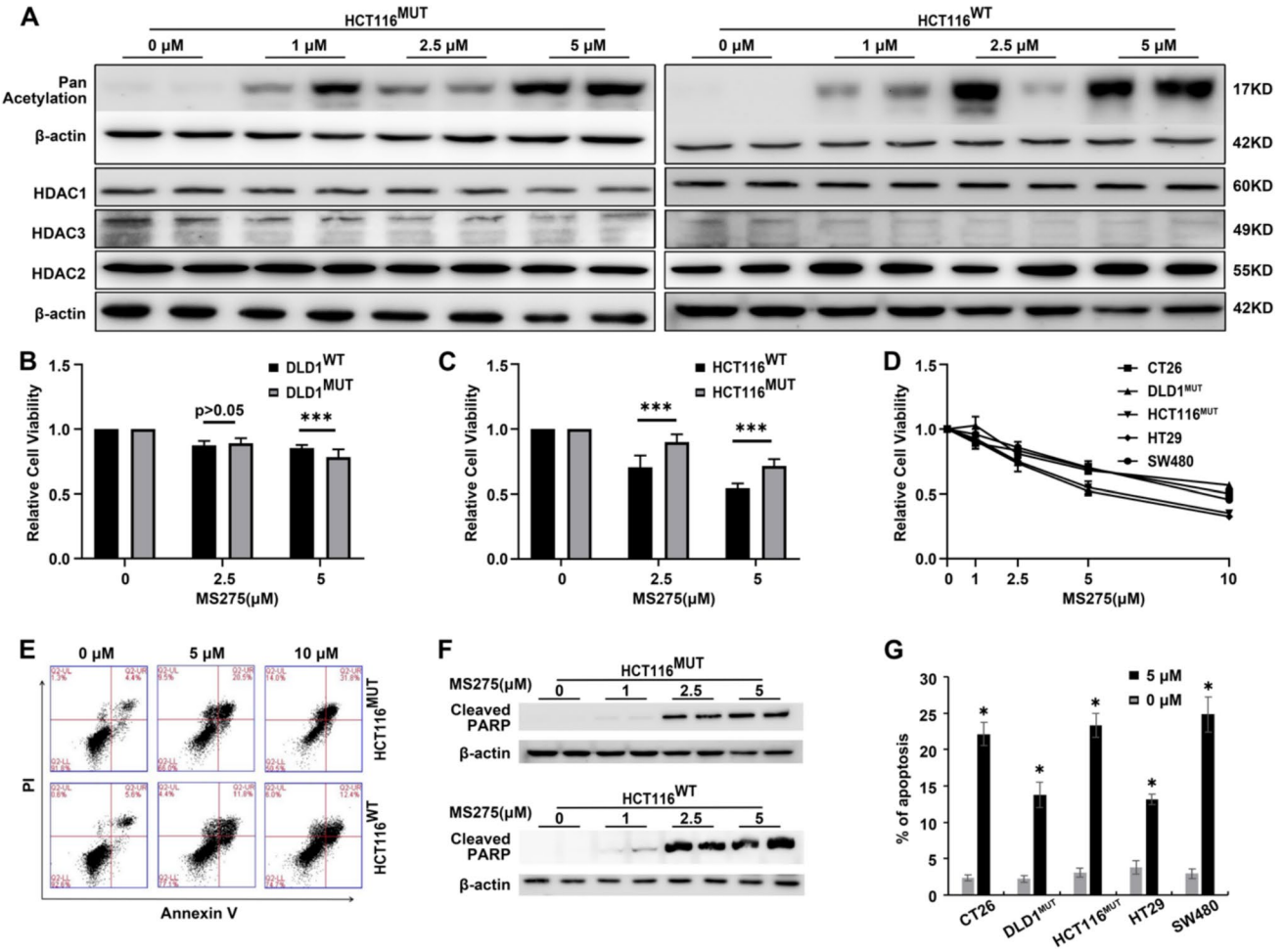

Fig. 1 MS275 inhibited proliferation, and induced apoptosis in colorectal cancer cells. **A** Western blot analysis of pan acetylation, HDAC1, HDAC2, and HDAC3 levels in CRC cells after treatment with increasing concentrations of MS-275. β-Actin levels were used as controls; The effect of MS275 on cell proliferation was evaluated in DLD1^{Mut} and DLD1^{WT} cells(**B**), in HCT116^{Mut} and HCT116^{WT} cells (**C**), and in a panel of CRC cell lines (**D**) was evaluated after treatment with MS275 for 48 h; **E** Apoptosis was examined using an Annexin V/PI assay; **F** The levels of cleaved PARP were determined by Western blot; **G** The effect of MS275-induced apoptosis was analyzed by flow cytometry in a panel of CRC cell lines after 48 h of incubation with MS275. $*p<0.05$, $***p<0.001$. Data plotted are mean ± SEM ($n=3$). DLD-1^{Mut} and HCT116^{Mut} cell lines contain the KRAS G13D mutation; DLD-1^{WT} and HCT116^{WT} are their isogenic cell lines carrying the wildtype KRAS

proliferation. In addition, TUNEL staining results indicated apoptosis of tumor tissues in the MS275-treated group (Fig. 2E), and the quantification analysis of BrdU and TUNEL is shown in Fig. 2F.

The orthotopic CRC models were established in both immunodeficient (nude) mice and immunocompetent (Balb/c) mice. After seven days of MS275 treatment, tumors were isolated for analysis. The results showed that MS275 treatment significantly inhibited tumor growth in both mouse models compared to the control group (Fig. 2G). The tumor-suppressive effect of MS275 was more pronounced in nude mice than in Balb/c mice with an intact immune system (Fig. 2H).

This suggests that MS275 could moderately inhibit the tumor establishment of colorectal tumors in mice, but not as effectively as observed in vitro.

MS275 treatment suppresses tumor immune microenvironment

AOM-DSS CRC tumor models were used to investigate the microenvironmental changes following MS275 administration. IHC staining revealed that F4/80-positive cells constituted the predominant infiltrating immune cells in the tumor microenvironment of the mouse colorectal cancer model, with fewer CD3 + T cells. The IHC scales of infiltrating

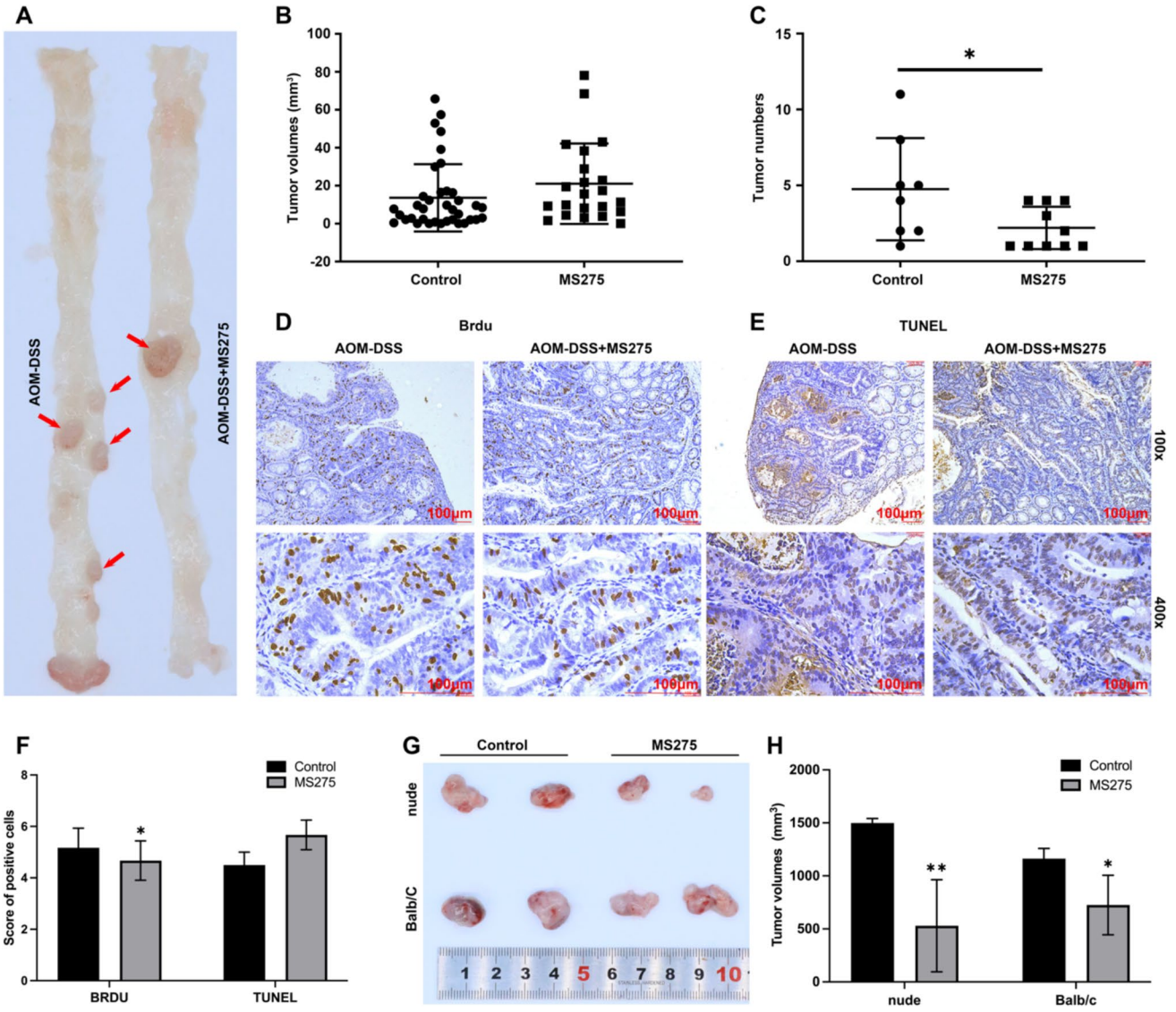

Fig. 2 MS275 inhibits AOM/DSS-induced CRC tumorigenesis. **A** Representative pictures of colon tumors in the different groups at week 14 after tumor initiation with/without MS275 treatment; Tumor volumes (**B**) and numbers(**C**) of AOM/DSS-treated mice (AOM/DSS) and AOM/DSS/MS275-treated mice (MS275); **D** Epithelial proliferation was measured via Brdu staining of the colon sections of mice (upper, ×100 magnification; lower, ×400 magnification); **E** Apoptosis was measured via TUNEL staining of the colon sections of mice (upper, ×100 magnification; lower, ×400 magnification); **F** the IHC quantification analysis of Brdu and TUNEL; **G** the effects of MS275 in immunodeficient (nude) mice and immunocompetent (Balb/c) mice; **H** tumor volumes of orthotopic tumor after MS275 treated in nude and Balb/c mice. $^{*}p < 0.05$, $^{**}p < 0.01$. Data plotted are mean ± SEM ($n \geq 3$)

immune cells, including F4/80 (Fig. 3A), CD3 + T cells (Fig. 3B), and CD8 + T cells (Fig. 3C), exhibited a reduction upon MS275 treatment. The results of the quantification analysis are shown in Fig. 3D.

Mesenteric lymph nodes (MLNs) are a crucial site for T cell activation in the colon. The pro-inflammatory cytokines TNF-α and IFN-γ were both upregulated in MLN isolated from AOM-DSS mice treated with MS275, indicating their potential role in tumor development (Fig. 3E).

Additionally, CD3 + T cells were isolated from the MLNs of AOM-DSS mice treated with MS275 using CD3 + magnetic bead sorting. The proportions of CD4 + and CD8 + T cells within the CD3 + T cell population were analyzed by FACS (Fig. 3F). The results demonstrated a significant increase in the proportion of CD3 + CD4 + T cells, while the proportion of CD3 + CD8 + T cells significantly decreased in the MS275 treatment group compared to the control group (Fig. 3G).

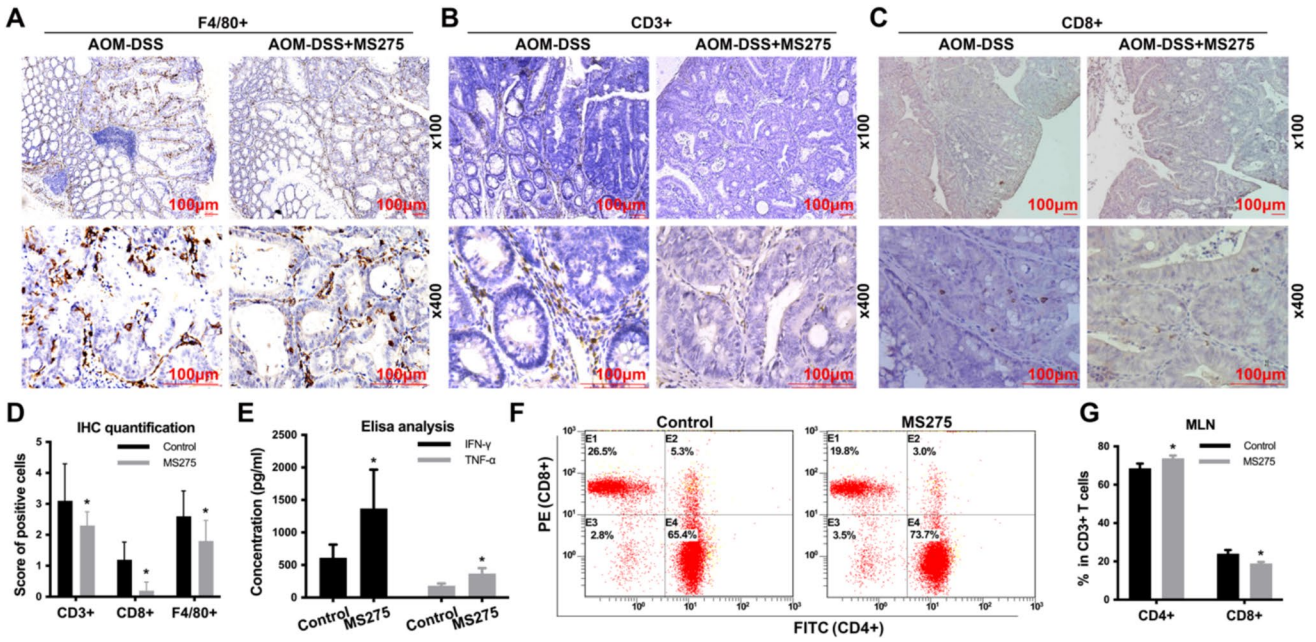

Fig. 3 MS275 treatment suppresses tumor immune microenvironment. **A**–**C** IHC features of tumor infiltrating immune/inflammatory cells. The representative photos are shown: F4/80(**A**), CD3 + T cells (**B**) and CD8 + T cells (C); **D** IHC quantification analysis for F4/80, CD3 + and CD8 + T cells; **E** IFN-γ and TNF-α concentrations in lymphocytes from MLN by ELISA; **F** Gated CD3 positive events were analyzed for CD4+ and CD8+ T cells distribution by FACS analysis in isolated cells of MLN; **G** The proportion of CD3 + CD4 + and CD3 + CD8 + T cells in MLN after MS275 treatment. $^{*}p < 0.05$. Data plotted are mean ± SEM ($n \geq 3$)

MS275 upregulated PD-L1 expression in colorectal cancer both in vitro and in vivo

To understand how MS275 reshapes the tumor microenvironment and its subsequent impact on the anti-tumor effect, we analyzed the effects of MS275 on PD-L1 expression in CRC cells. Following treatment with MS275, qRT-PCR (Fig. 4A–C) and Western blotting assays (Fig. 4D–F) revealed an upregulation of PD-L1 at both the mRNA and protein levels. These findings were further confirmed by evaluating PD-L1 expression using flow cytometry (Fig. 4G).

The ability of MS275 to upregulate PD-L1 in vivo was also investigated in tumor tissue from the AOM-DSS CRC model. After treatment with MS275, PD-L1 expression in the tumors was assessed by Western blotting. Consistent with the in vitro data, MS275 treatment significantly increased PD-L1 expression in tumors (Fig. 4H).

To determine whether the upregulation of PD-L1 is specifically mediated through HDAC inhibition, HDAC1, HDAC2, and HDAC3 were individually knocked down using shRNA. Compared to the negative control, the upregulation of PD-L1 was specifically associated with decreased HDAC3 expression and was not affected by the knockdown of HDAC1 or HDAC2 (Fig. 4I).

Anti-tumor effects of MS275 in combination with an anti-PD-1 antibody

Given that MS275 inhibits tumor immune response by upregulating PD-L1 expression in tumor cells, we further explored the possibility of enhancing the anticancer effect of MS275 by blocking the PD-1/PD-L1 signaling pathway using a PD-1 monoclonal antibody.

In AOM-DSS CRC model mice, we evaluated the anti-tumor effects following 3 weeks of treatment with both MS275 (20 mg/kg/day) and PD-1 monoclonal antibody (5 mg/kg/3 days). The results showed that the co-treatment significantly enhanced the inhibitory effect on tumor growth compared to treatment with MS275 alone (Fig. 5A). The numbers of tumors in the combination treatment group were significantly decreased compared to the control or MS275/PD-1 single treatment group (Fig. 5B). While treatment with either MS275 or PD-1 monoclonal antibody alone tended to reduce tumor volumescompared to the control group. The combination of MS275 and PD-1 monoclonal antibody treatment led to the most significant tumor suppression, with lower tumor volumes than those observed with either treatment alone (Fig. 5C).

The proliferation or apoptosis was assessed after administration with either MS275 or PD-1 monoclonal antibody

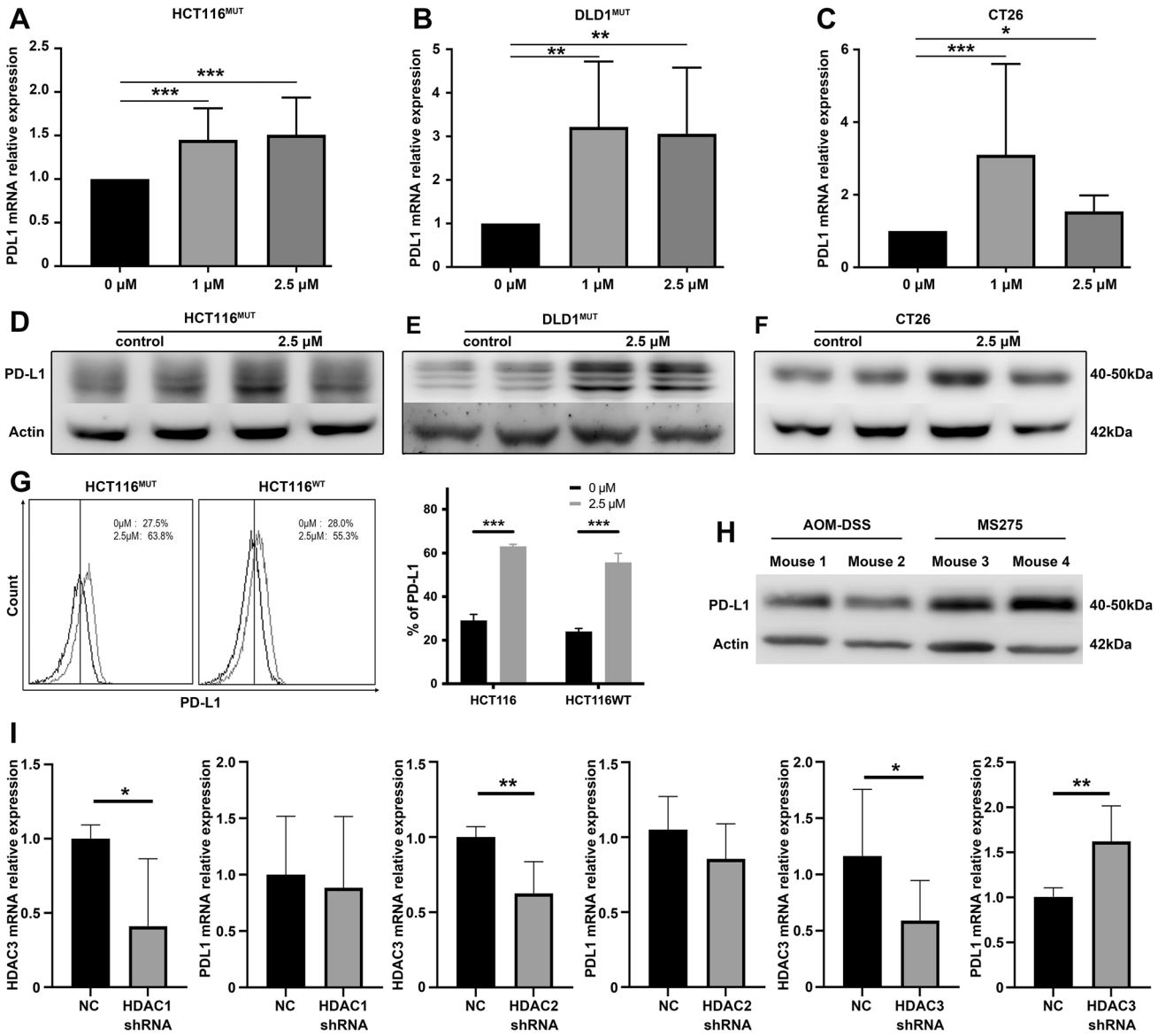

Fig. 4 MS275 upregulated PD-L1 expression in colorectal cancer. q-RT-PCR of PD-L1 in CRC cells HCT116^{MUT}(**A**), DLD1^{MUT}(**B**) and CT26(**C**) treated with MS275 for 24 h, GAPDH as controls; Western blot analysis of PD-L1 expression in CRC cells HCT116^{MUT}(**D**), DLD1^{MUT}(**E**) and CT26 (**F**) treated with MS275 (2.5 μM) for 24 h, β-actin as controls; **G** FACS analysis of cell-surface expression of PD-L1 in colorectal cancer cells following MS275 treatment for 24 h; **H** Western blot analysis of PD-L1 expression in tumor from AOM-DSS CRC model with/without MS275 treatment for 3 weeks; **I** qRT-PCR was performed to evaluate the knockdown efficiency of HDAC1, HDAC2, and HDAC3. Additionally, the expression levels of PD-L1 were assessed following the knockdown of each HDAC. *$p<0.05$; **$p<0.01$ and ***$p<0.001$. Data plotted are mean ± SEM ($n \geq 3$)

alone or in combination. BrdU staining demonstrated that intra-tumoral proliferation rates were decreased after MS275 and PD-1 co-treatment, suggesting that the combination treatment inhibits epithelial proliferation (5D). In contrast, TUNEL staining revealed that the combination treatment increased intra-tumoral apoptosis, in comparison to the control and single treatment groups (Fig. 5E).

The IHC scales of infiltrating immune cells, including CD3 + T cells (Fig. 5F) and CD8 + T cells (Fig. 5G) exhibited an increase upon MS275 and PD-1 co-treatment. There was an overall reduction in the number of F4/80 cells infiltrating the tumors in combination treatment (Fig. 5H).

CD3 + T cells isolated from the MLNs of AOM-DSS mice that have been administrated with MS275/PD-1 single or co-treatment. The results demonstrated that CD8 + CD3 + T cells increased and CD4 + CD3 + T cells decreased in the combination treatment group compared to the control or single treatment groups. The data were shown in Fig. 5I, J.

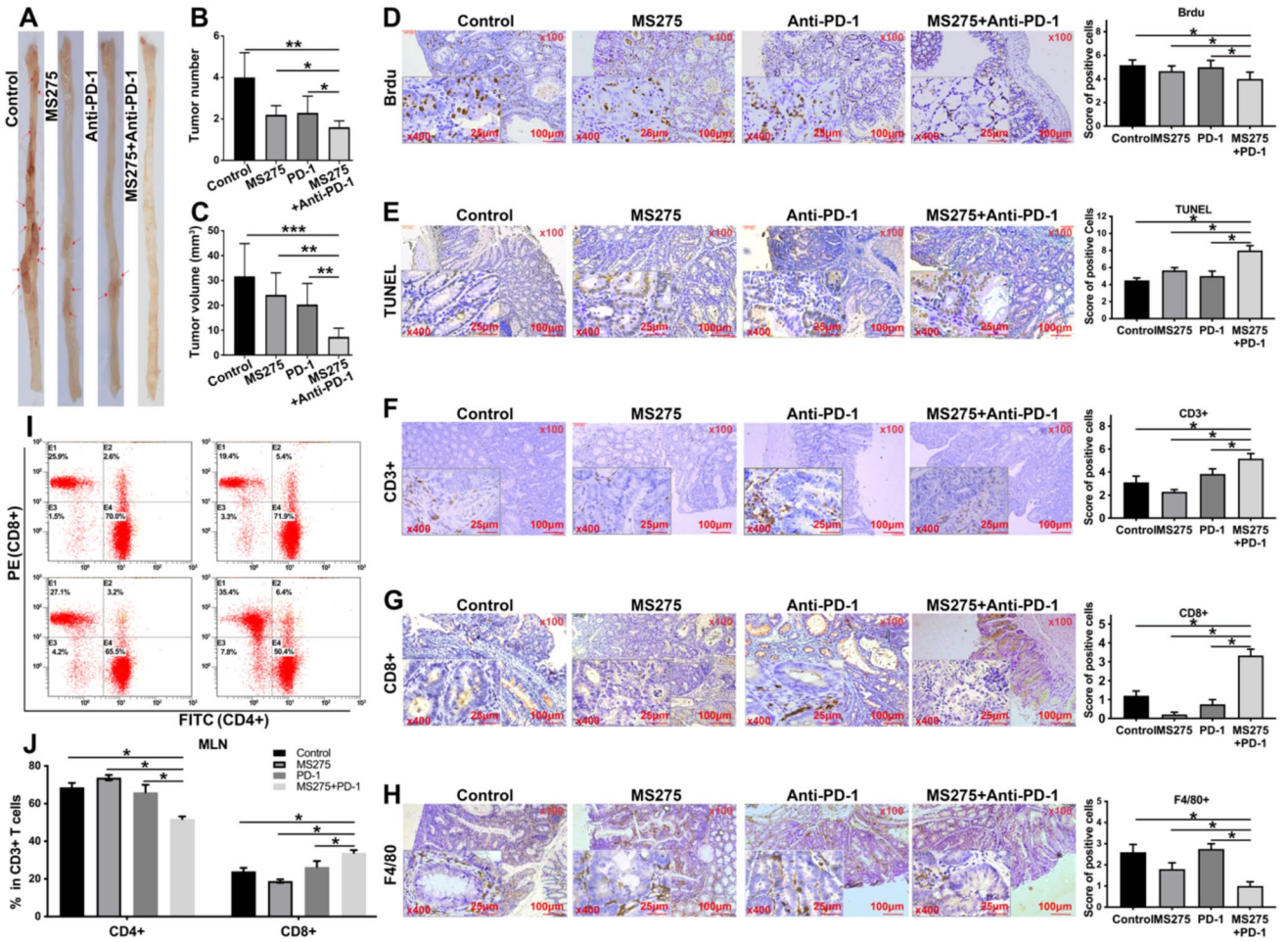

Fig. 5 Enhanced anti-tumor efficacy through co-treatment with MS275 and PD-1 mono antibody. **A** Representative pictures of colon tumors in AOM-DSS mouse model with MS275/PD-1 alone or together treatment. Tumor numbers (**B**) and volumes (**C**) of colon tumors in AOM-DSS mouse model with MS275/PD-1 alone or co-treatment; **D** Brdu staining for proliferation of the colon sections of mice (×100 and ×400 magnification); **E** Apoptosis was measured via TUNEL staining of the colon sections of mice (×100 and ×400 magnification); Representative CD3 + (**F**), CD8 + (**G**), and F4/80(**H**) staining and quantification for tumor infiltrating lymphocytes, ×100 and × 400 magnification; **I** Gated CD3 positive events were analyzed for CD4 and CD8 distribution by FACS analysis in isolated cells of MLN; **J** The proportion of CD3 + CD4 + and CD3 + CD8 + cells in MLN after indicated treatment. $*p < 0.05$; $**p < 0.01$ and $***p < 0.001$. Data plotted are mean ± SEM ($n > 3$)

Stat3 activation is required for MS275 upregulation of PD-L1 in colorectal cancer cells

It is well-known that HDACi has close relationship with STAT3 activation in gut epithelial cells [10] and in a murine Lewis lung carcinoma model [11]. To elucidate if MS275 regulates PD-L1 transcriptionally, we assessed phosphorylated STAT3 protein levels in colorectal cell lines and a CRC mouse model.

MS275 significantly upregulated the expression levels of phosphorylated STAT3 protein in HCT116^{Mut} and HCT116^{WT} cell lines, along with increased PD-L1 expression (Fig. 6A). The same results were obtained in the AOM-DSS CRC mouse model (Fig. 6B–D). The phosphorylated Stat3 was increased in MS275 and anti PD-1 co-treatment group compared with the control group (Fig. 6C).

The role of STAT3 in the regulation of PD-L1 was investigated using the STAT3 inhibitor, Stattic. HCT116^{Mut} cells were treated with Stattic(5 μM) for indicated time point for blocking phosphorylated STAT3, the gene expression of PD-L1 was observed to increase as early as 0.5 h after treatment (Fig. 6E).

Pre-treatment of CRC cells with Stattic(5 μM) for 60 min, phosphorylated STAT3 in both HCT116^{Mut} and HCT116^{WT} cell lines were inhibited. The levels of PD-L1 protein expression remained unchanged following subsequent treatment with MS275 and stattic for 24 h (Fig. 6F–H). These results suggest that activated STAT3 is likely a central regulator of PD-L1 expression by MS275.

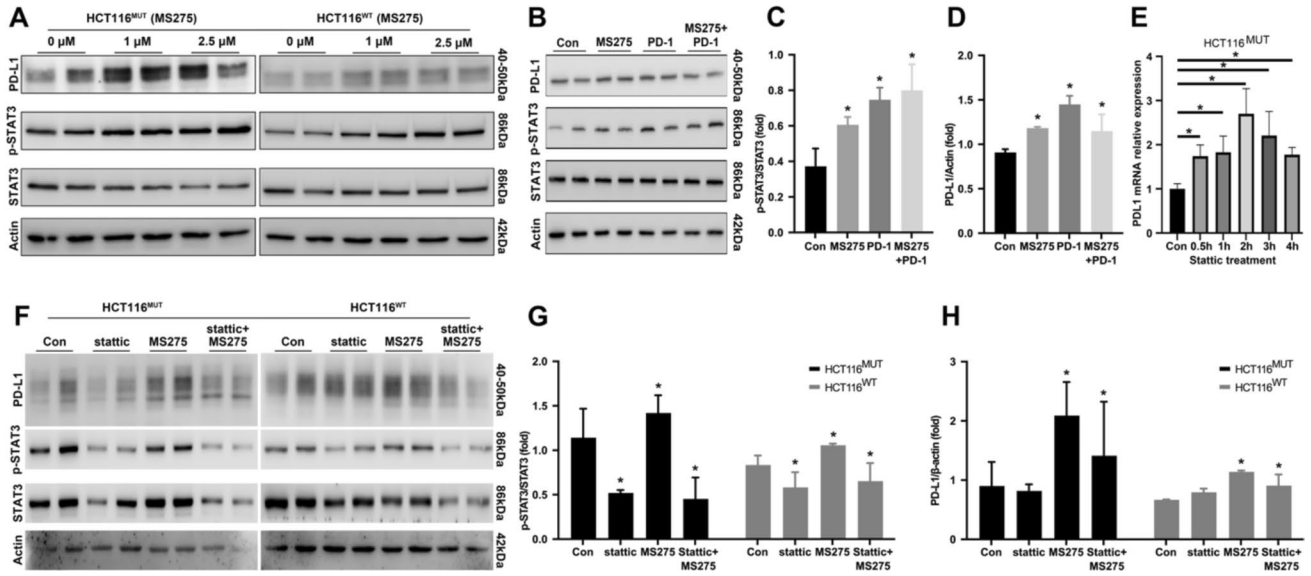

Fig. 6 MS275 increased PD-L1 expression by activating STAT3 **A** Western blot analysis of STAT3 phosphorylation in CRC cells treated with MS275 for 24 h, β-actin levels as controls; **B** Representative STAT3 phosphorylation a of colon tumors in AOM-DSS mouse model with MS275/PD-1 alone or together treatment; **C** and **D** Quantitative analysis of phosphorylated STAT3 in AOM-DSS mouse model with MS275/PD-1 alone or together treatment; **E** q-RT-PCR of PD-L1 in CRC cells HCT116^{MUT}treated with MS275 (2.5 μM) for indicated time point, GAPDH as controls **F** Western blot analysis was performed to assess Stat3 phosphorylation in CRC cells pre-treated with Stattic (5 μM) for 1 h, followed by treatment with MS275 for 24 h; **G** and **H** Quantitative analysis of phosphorylated STAT3 and PD-L1 in CRC cells treated with MS275/Stattic for 24 h $^*p<0.05$. Data plotted are mean ± SEM ($n=3$)

Discussion

MS275, a benzamide that specifically inhibits class I HDAC, has shown preclinical anti-tumor effects in a variety of cancers, including colorectal cancer, breast cancer, hematological malignancies [12], and others. Consistent with previous studies, our study also confirmed that MS275 can inhibit proliferation and viability and promote apoptosis in colorectal cancer cells. Besides apoptosis, MS275 can induce various forms of cell death, including cell cycle arrest, autophagy, and necrosis [13]. This may explain why MS275 showed inconsistent effects on apoptosis and cell viability in different cell lines, shown in Fig. 1C. KRAS is a well-known mutation in CRC. Prior reports have indicated that Ras mutations may render lung cancer cells more susceptible to HDAC inhibitor treatment [14, 15]. However, our data demonstrated that MS275's inhibitory effect on colorectal cancer cells was independent of the KRAS gene mutations present in the cells. This suggests that MS275 would be valuable in treating a larger subset of patients.

However, the inhibition of tumor growth by MS275 in the AOM-DSS CRC mouse model was not as effective as observed in vitro. Our data showed that the tumor-suppressive effect of MS275 was more pronounced in immune-deficient mice compared to immune-competent mice in the orthotopic CRC model. The efficacy of MS275 as a single agent therapy remains limited [16]. In a phase II study of MS275 monotherapy in relapsed/refractory Hodgkin lymphoma, the overall response rate was modest (12%)[17]. Studies have explored strategies to combine MS275 with other drugs to enhance therapeutic outcomes. For instance, traditional chemotherapy drugs like 5-fluorouracil (5-FU) [18], and oxaliplatin [19, 20] were combined with MS275 to augment chemotherapy efficacy. Additionally, combining MS275 with inhibitors targeting the EGFR pathway (such as cetuximab or panitumumab) in CRC [21] or with HER2-targeted therapies in breast cancer [22] may enhance anti-tumor effects. Furthermore, MS275 may be combined with other epigenetic modifiers. However, the clinical phase outcomes of these combinations have not met expectations. The combination of regorafenib, HCQ, and MS275 was poorly tolerated without evident activity in metastatic CRC [6].

In addition to directly suppressing tumor cells, HDAC inhibitors have been reported to modulate the immune system [5, 23, 24]. We also found a reduction in CD3 + T cell tumor infiltration following MS275 treatment. Moreover, levels of the pro-inflammatory cytokines TNF-α and IFN-γ were both increased in mesenteric lymphocytes isolated from AOM-DSS mice treated with MS275. Because mesenteric lymph nodes (MLNs) are sentinel sites of enteral immune surveillance and immune homeostasis [25] and are an important site for T cell activation in the colon [26], CD3 + T cells were isolated from the MLN and the percentage of CD4 + T cells and CD8 + T cells among CD3 + T cells

was determined after treatment. The results showed a significant decrease in the proportion of CD3 + CD8 + T cells and an increase in the proportion of CD3 + CD4 + T cells in MLN from MS275-treated AOM-DSS tumors. The enhancement of immune suppression by MS275 and its contribution to tumor immune escape elucidate the diminished efficacy of MS275 in vivo relative to in vitro. This, in turn, gives rise to tumor immune tolerance or escape, thereby constraining its utility in clinical treatment.

Immune checkpoints play a crucial role in regulating tumor immune environments. Among them, the upregulation of PD-1/PD-L1 has gained significant attention due to its role in immune suppression, making it a prominent target for tumor immunotherapy. Accumulating evidence indicates that HDAC activation could induce PD-L1 expression in various types of cancer [27]. We also found that PD-L1 is upregulated on tumor cells following MS275 treatment. Furthermore, the combination of MS275 with anti-PD-1 in AOM-DSS mouse tumor models resulted in increased CD3 + T cells and CD8 + T cells infiltration. Furthermore, the proportion of CD8 + T cells increased and that of CD4 + T cells decreased among CD3 + positive T cells in the mesenteric lymph nodes (MLN), which are a crucial site for T cell activation in the colon. The mechanism of reprogramming immunosuppressive responses via MS275 is not clear. As a histone deacetylase inhibitor, MS275 can regulate the anti-tumor immunity by epigenetically modifying genes in cancer cells, potentially enabling cancer cells to evade the immune surveillance. Additionally, MS275 may directly affect immune cell activity by reducing the activation of monocytes, alleviating T cell exhaustion or increasing immune checkpoint receptor expression. Further studies are needed to investigate the direct systemic effects of MS275 on immune cells as well as its specific effects mediated by cancer cells.

Although inhibition of class I HDACs has been associated with increased PD-L1 expression [5, 28], the precise mechanism of PD-L1 regulation remains unclear. Our research demonstrated that treatment with MS275 led to elevated levels of STAT3 phosphorylation in mouse CRC tissues and cultured cells. The expression of PD-L1 was observed to decrease in response to the downregulation of phosphorylated STAT3 by the inhibitor Stattic. These findings align with those previously reported by the Kim Y. group, which showed that inhibiting Stat3 activation can downregulate PD-L1 expression in a murine Lewis lung carcinoma model [11]. Collectively, these results suggest that STAT3-mediated transcriptional activation by MS275 may contribute to the upregulation of PD-L1.

In CRC, the balance between anti-tumoral and pro-tumoral immune functions is largely dependent on the level of PD-L1 expression. CRC with both high PD-1 and PD-L1 levels may have an active immune checkpoint activity and may therefore represent the subset that benefits from anti-PD-1 therapy [29]. However, the overall response rates to PD-1 inhibitors in CRC remain modest, with only a subset of patients experiencing durable responses [30]. Although the upregulation of PD-L1 following MS275 treatment negatively regulates T cell responses and facilitates immune escape, emerging evidence suggests that MS275-induced upregulation of PD-L1 can improve the efficacy of anti-PD-1 immunotherapy. This highlights the potential for combining MS275 with anti-PD-1 therapy as an effective strategy to enhance immunotherapy efficacy in CRC.

Acknowledgements We thank Dr.Ling GU for providing for useful discussion. We thank the National Natural Science Foundation of China for its support.

Author contributions YF.W. and J.Z designed the research; D.T, ZG.M and SH.C, carried out most of the experiments; M.S., M.L, Q.X, RT.Y and XX. Z provided extra technical assistance; SQ.L, M.L, M.S.,D.T., Q.X, and RT.Y performed material preparation; the first draft of the manuscript was written by YF.W. and J.Z. and all authors commented on previous versions of the manuscript. All authors read and approved the final manuscript.

Funding This work was supported by grants from the National Natural Science Foundation of China (Grant Nos. 82173104 and 81871233).

Data availability No datasets were generated or analysed during the current study.

Declarations

Conflict of interest The authors declare no competing interests.

Ethical approval All animal experiments were performed in line with International Guidelines and Protocols. This study and included experimental procedures were approved by the Institutional Animal Care and Use Committee of Sichuan University. All animal housing and experiments were conducted in strict accordance with the institutional guidelines for care and use of laboratory animals.

Consent to participation None.

Consent for publication Not applicable.

References

1. Garmpis N et al (2022) Histone deacetylases and their inhibitors in colorectal cancer therapy: current evidence and future considerations. Curr Med Chem 29:2979–2994. https://doi.org/10.2174/0929867328666210915105929
2. Li Y, Seto E (2016) HDACs and HDAC inhibitors in cancer development and therapy. Cold Spring Harb Perspect Med. https://doi.org/10.1101/cshperspect.a026831
3. Mariadason JM (2008) HDACs and HDAC inhibitors in colon cancer. Epigenetics 3:28–37. https://doi.org/10.4161/epi.3.1.5736
4. Mayer M et al (2022) Preclinical efficacy and toxicity analysis of the pan-histone deacetylase inhibitor gossypol for the therapy of colorectal cancer or hepatocellular carcinoma. Pharmaceuticals. https://doi.org/10.3390/ph15040438
5. Blaszczak W et al (2021) Immune modulation underpins the anticancer activity of HDAC inhibitors. Mol Oncol 15:3280–3298. https://doi.org/10.1002/1878-0261.12953
6. Karasic TB et al (2022) Phase I trial of regorafenib, hydroxychloroquine, and entinostat in metastatic colorectal cancer. Oncologist 27:716-e689. https://doi.org/10.1093/oncolo/oyac078
7. Hess-Stumpp H, Bracker TU, Henderson D, Politz O (2007) MS-275, a potent orally available inhibitor of histone deacetylases–the development of an anticancer agent. Int J Biochem Cell Biol 39:1388–1405. https://doi.org/10.1016/j.biocel.2007.02.009
8. Connolly RM, Rudek MA, Piekarz R (2017) Entinostat: a promising treatment option for patients with advanced breast cancer. Future Oncol 13:1137–1148. https://doi.org/10.2217/fon-2016-0526
9. Bracker TU et al (2009) Efficacy of MS-275, a selective inhibitor of class I histone deacetylases, in human colon cancer models. Int J Oncol 35:909–920. https://doi.org/10.3892/ijo_00000406
10. Zheng L et al (2017) Microbial-derived butyrate promotes epithelial barrier function through IL-10 receptor-dependent repression of claudin-2. J Immunol 199:2976–2984. https://doi.org/10.4049/jimmunol.1700105
11. Kim Y et al (2022) Immunomodulation of HDAC inhibitor entinostat potentiates the anticancer effects of radiation and PD-1 blockade in the murine Lewis lung carcinoma model. Int J Mol Sci. https://doi.org/10.3390/ijms232415539
12. Vire B et al (2009) Anti-leukemia activity of MS-275 histone deacetylase inhibitor implicates 4–1BBL/4-1BB immunomodulatory functions. PLoS ONE 4:e7085. https://doi.org/10.1371/journal.pone.0007085
13. Mrakovcic M, Kleinheinz J, Frohlich LF (2017) Histone deacetylase inhibitor-induced autophagy in tumor cells: implications for p53. Int J Mol Sci. https://doi.org/10.3390/ijms18091883
14. Eichner LJ et al (2023) HDAC3 is critical in tumor development and therapeutic resistance in Kras-mutant non-small cell lung cancer. Sci Adv 9:eadd3243. https://doi.org/10.1126/sciadv.add3243
15. Peter RM et al (2023) Histone deacetylase inhibitor belinostat regulates metabolic reprogramming in killing KRAS-mutant human lung cancer cells. Mol Carcinog 62:1136–1146. https://doi.org/10.1002/mc.23551
16. Gojo I et al (2007) Phase 1 and pharmacologic study of MS-275, a histone deacetylase inhibitor, in adults with refractory and relapsed acute leukemias. Blood 109:2781–2790. https://doi.org/10.1182/blood-2006-05-021873
17. Batlevi CL et al (2016) ENGAGE- 501: phase II study of entinostat (SNDX-275) in relapsed and refractory Hodgkin lymphoma. Haematologica 101:968–975. https://doi.org/10.3324/haematol.2016.142406
18. Flis S, Gnyszka A, Flis K, Splawinski J (2010) MS275 enhances cytotoxicity induced by 5-fluorouracil in the colorectal cancer cells. Eur J Pharmacol 627:26–32. https://doi.org/10.1016/j.ejphar.2009.10.033
19. Flis S, Gnyszka A, Splawinski J (2009) HDAC inhibitors, MS275 and SBHA, enhances cytotoxicity induced by oxaliplatin in the colorectal cancer cell lines. Biochem Biophys Res Commun 387:336–341. https://doi.org/10.1016/j.bbrc.2009.07.017
20. Lamoine S et al (2021) The class I HDAC inhibitor, MS-275, prevents oxaliplatin-induced chronic neuropathy and potentiates its antiproliferative activity in mice. Int J Mol Sci. https://doi.org/10.3390/ijms23010098
21. Jenke R, Ressing N, Hansen FK, Aigner A, Buch T (2021) Anticancer therapy with HDAC inhibitors: mechanism-based combination strategies and future perspectives. Cancers. https://doi.org/10.3390/cancers13040634
22. Christmas BJ et al (2018) Entinostat converts immune-resistant breast and pancreatic cancers into checkpoint-responsive tumors by reprogramming tumor-infiltrating MDSCs. Cancer Immunol Res 6:1561–1577. https://doi.org/10.1158/2326-6066.CIR-18-0070
23. Smith HJ et al (2018) The antitumor effects of entinostat in ovarian cancer require adaptive immunity. Cancer 124:4657–4666. https://doi.org/10.1002/cncr.31761
24. Yelton CJ, Ray SK (2018) Histone deacetylase enzymes and selective histone deacetylase inhibitors for antitumor effects and enhancement of antitumor immunity in glioblastoma. Neuroimmunol Neuroinflamm. https://doi.org/10.20517/2347-8659.2018.58
25. Shaikh H et al (2021) Mesenteric lymph node transplantation in mice to study immune responses of the gastrointestinal tract. Front Immunol 12:689896. https://doi.org/10.3389/fimmu.2021.689896
26. Houston SA et al (2016) The lymph nodes draining the small intestine and colon are anatomically separate and immunologically distinct. Mucosal Immunol 9:468–478. https://doi.org/10.1038/mi.2015.77
27. Liu X et al (2020) HDAC10 is positively associated with PD-L1 expression and poor prognosis in patients with NSCLC. Front Oncol 10:485. https://doi.org/10.3389/fonc.2020.00485
28. Hegedus L et al (2020) HDAC inhibition induces PD-L1 expression in a novel anaplastic thyroid cancer cell line. Pathol Oncol Res 26:2523–2535. https://doi.org/10.1007/s12253-020-00834-y
29. Cui G (2021) The mechanisms leading to distinct responses to PD-1/PD-L1 blockades in colorectal cancers with different MSI statuses. Front Oncol 11:573547. https://doi.org/10.3389/fonc.2021.573547
30. Payandeh Z et al (2020) PD-1/PD-L1-dependent immune response in colorectal cancer. J Cell Physiol 235:5461–5475. https://doi.org/10.1002/jcp.29494